Electrical burst signature of pore-scale displacements

A. Haas[1] and A. Revil[1,2]

Received 1 May 2009; revised 31 July 2009; accepted 25 August 2009; published 16 October 2009.

[1] Electric field bursts were passively observed when a nonwetting fluid displaced a wetting fluid in a porous material (drainage) as well as during imbibition experiments. A sandbox experiment was conducted to study these electrical disturbances using a network of very sensitive nonpolarizing electrodes located at the top surface of the tank. Drainage exhibited many more electrical bursts, with a higher magnitude, than imbibition. These events were only observed during drainage or imbibition, not prior to or after the water flowed inside the porous sandbox. We point out the possible relationship between the formation of Haines jumps and the occurrence of these electrical bursts. These bursts show a power law distribution during drainage with a power law exponent of about −1.7, in agreement with a previous published study using acoustic and hydroacoustic events. Imbibition does not display such a power law relationship.

Citation: Haas, A., and A. Revil (2009), Electrical burst signature of pore-scale displacements, *Water Resour. Res.*, *45*, W10202, doi:10.1029/2009WR008160.

1. Introduction

[2] Drainage of a porous media initially saturated with a wetting phase like water with a nonwetting phase like air takes place under a process called invasion percolation [*Aker et al.*, 2000; *Crandall et al.*, 2009]. In a granular material like sand, large pores are connected by smaller throats. The invading nonwetting fluid (air) will get held up at the throats between the pores where the capillary forces are greatest. As the wetting phase (water in the experiments reported below) is continuously removed from below, the air-water interface at the throat with the largest radius will become unstable. Finally, when the capillary entry pressure of the throat is exceeded, the throat and the pore below the throat spontaneously fill with air. All of the larger pores connected to the newly filled pore through throats that are of the same size or larger also fill with air. The air-water interface then restabilizes at throats behind the pore that are smaller than the initial throat that gave way. Consequently, if one or many of the other throats connected to the newly filled pore are larger than the initial throat holding the interface, these throats and subsequent pores spontaneously fill with the nonwetting phase also. Therefore, once the interface at a particular throat becomes unstable, it causes an avalanche of pore and throat fillings with air that will only stop at throats smaller than the first throat. This jump of the position of the meniscus is called a Haines jump [*Haines*, 1930; *Aker et al.*, 2000; *Crandall et al.*, 2009].

[3] Imbibition is also characterized by Haines jumps. However, imbibition is a collective process because water is the wetting fluid, capillary forces will hold up the invading water at the large pores. Once a pore fills, all of the throats connected to that pore fill as they are smaller in size. However, during imbibition, even if a small pore lies behind a large pore, the small pore may not spontaneously fill after the filling of the large pore. This limits the size of the potential avalanches during imbibition when compared to drainage. Another process called "snap off" is also acting during imbibition to decrease the size of the avalanches. This is caused by water moving along the edges of the pore space, allowing small throats ahead of the wetting front to fill spontaneously [*Tuller and Or*, 2001]. These filling events would consist of a single throat and may therefore not emit enough energy to be detectable.

[4] The self-potential method [e.g., *Jardani et al.*, 2008, 2009] is a passive electrical method in which the fluctuations of the electrical potential associated with in situ sources of electrical currents is recorded using a set of electrodes. This is also what is done in electroencephalography. In electroencephalography, a network of electrodes is applied to the scalp and used to detect/locate the source of brain activity. The brain activity is associated with the generation of tiny electrical currents at the synapses between neurons when ionic channels are enabled to allow the transport of ionic compounds.

[5] It is reasonable to assume that Haines jumps should generate electrical current bursts. Indeed, in a porous material all minerals in contact with water develop a surface charge through chemical reactions. Part of this charge is neutralized by sorption of counterions in the so-called Stern layer. The neutrality is achieved by the presence of an excess of charge in the vicinity of the mineral surface through Coulombic interaction with the charge attached to the mineral framework. This process is known as the electrical double layer. It implies that the pore water carries a net amount of charge, generally positive [*Leroy et al.*, 2007]. The displacement of this positive charge by the flow of the pore water is equivalent to a source of current (charge moving per unit surface area per unit time) called the streaming current. The associated electrical field is called the streaming potential.

[1]Department of Geophysics, Colorado School of Mines, Golden, Colorado, USA.
[2]Equipe Volcans, LGIT, UMR 5559, INSU, Université de Savoie, CNRS, Le Bourget du Lac, France.

0043-1397/09/2009WR008160$09.00

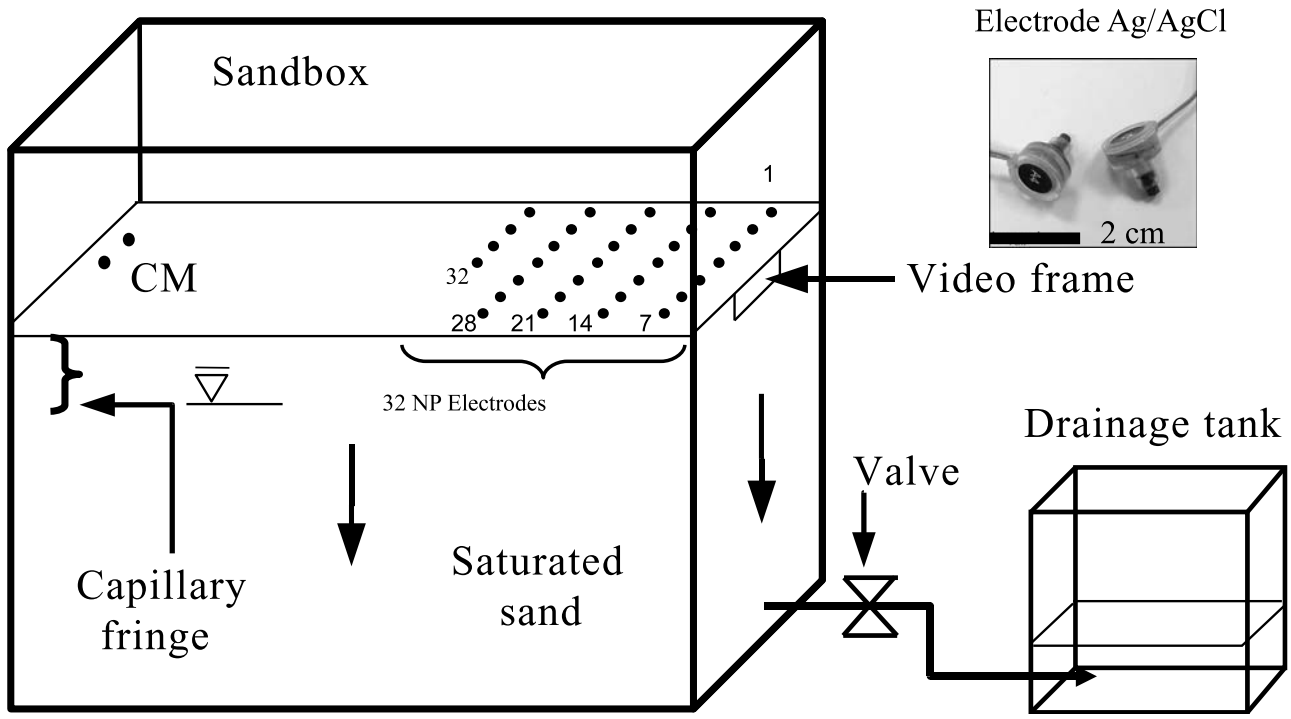

Figure 1. Sketch of the experiment. The sandbox is filled with sand saturated by tape water. CM corresponds to the common mode range control node (reference) of the nonpolarizing (NP) electrodes. The nonpolarizing electrodes are Ag/AgCl electrodes with amplifiers. All the electrical potentials are recorded relative to the potential of the reference (CM) electrode.

[6] In the present paper, we are looking to observe, for the first time, streaming potentials associated with Haines jumps, and briefly compare the electrical burst trends we observed with acoustic burst trends previously studied by *DiCarlo et al.* [2003]. A test apparatus, initially developed for electroencaphalography, was used by *Crespy et al.* [2008] to observe in real time the spatial distribution of very small voltages over the surface of a saturated sandbox during very small fluid pumping and infiltration tests. In the present paper, we apply this approach to detect the dynamic electrical bursts potentially associated with Haines jumps during drainage and imbibition experiments.

2. Material and Methods

[7] The test system consisted of a 20 gallon (0.075 m^3) sandbox filled with an unconsolidated sand (mean diameter in the range 425–600 μm) filled to saturation with tap water (electrical resistivity of 650 ohm m at 25°C, measurements made at 22°C). The data acquisition system was composed of 32 amplified nonpolarizing silver–silver chloride electrodes placed on a 5.1 cm by 5.1 cm grid forming a 5 × 7 network of electrodes at the top surface of the sandbox (Figure 1). The data acquisition system was a self-contained, battery powered, galvanically isolated, digitally multiplexed, amplified electrode, high-sensitivity voltage measurement system with a single analog to digital converter per measurement channel. The measurement system had a 24 bit resolution with a sample rate of 2,048 Hz having an overall response of DC to 400 Hz (system filtered). The digitization part of the system had a sampling process with <10 ps skew among channels and 200 ps sample rate jitter. The digitally multiplexed signals were subsequently serialized into a bit wide data stream and sent through a fiber-optic cable (to achieve galvanic isolation) to a USB based computer interface.

[8] The scaled quantization level was 31.25 nV (LSB) with 0.8 μV RMS noise (5 μV peak to peak) full bandwidth. The amplified nonpolarizing electrode input impedance is 300 MΩ at 50 Hz (see *Crespy et al.* [2008] for further explanations). The voltage reference for the measurements was contained within the measurement area, and was designed into the measurement system as a common mode range control and voltage reference (CM in Figure 1). All voltages measured by this system are relative to the CM electrode. The entire system, including the computer was operated on batteries to minimize conductive coupling with the electrical power system.

[9] After turn on, the electronics was allowed to stabilize thermally for about 15 min. This minimized the thermal drift in the signal due to electronics temperature stabilization. The electrodes were also allowed to stabilize during this time. Additionally, the experiment was accomplished relatively quickly, typically less than 5 min, and the thermal mass of the sand and water was very large and responds very slowly relative to any room temperature fluctuations.

[10] The gravity driven drainage started by turning on the control valve, allowing water to flow out of the main tank into the drainage tank (the opposite for imbibition). The drainage tube (0.6 cm vinyl tube) was connected near the bottom of the main tank and near the bottom of the drainage tank (Figure 1). Water was imbibed into or drained from the

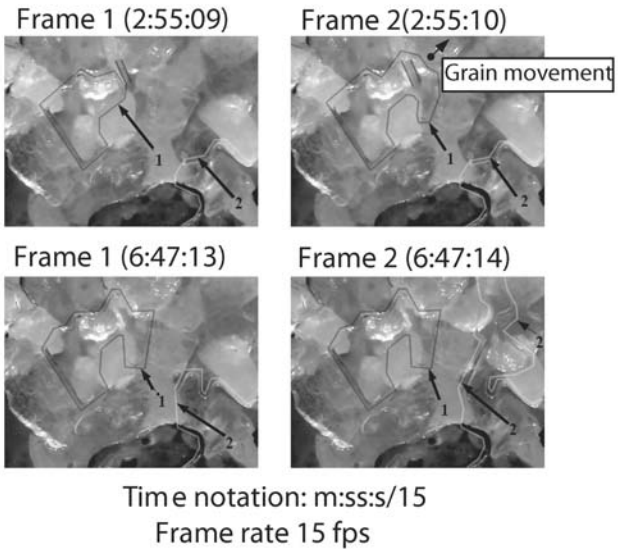

Figure 2. Haines jumps. (top) Pictures showing instabilities in the position of the meniscus (outlined by solid lines) during drainage. The two pictures show that the meniscus labeled 1 is jumping while the meniscus labeled 2 is stable. (bottom) The opposite situation (fps stands for frames per second).

sand through a porous body at the bottom of the sandbox. In the drainage experiment, the head difference between the saturated surface of the sand and the water level in the drainage tank was 30.5 cm.

[11] A MATLAB code was written to read the data file generated by the voltage measurement system (BDF file format), perform digital signal processing (DSP, using various functions from the MATLAB signal processing toolbox, MSPT), reorganize the data into the relative physical electrode locations, and display it in a variety of graphical formats for visual analysis. The DSP portion of the code was accomplished on a channel by channel basis and included DC normalization (not with MSPT), window function application for Fourier transform analysis, Butterworth based infinite impulse response (IIR) narrow band reject filtering (to suppress 60 Hz and related harmonics), and a high-order linear phase finite impulse response (FIR) 1 Hz high-pass filter for low-frequency trend removal process. MATLAB nonlinear curve fitting tools were used to generate the fits to the threshold counted data.

[12] The post data acquisition signal processing and analysis sequence is as follows: (1) the data in the BDF file is read into memory; (2) a single channel was selected and used to perform spectral analysis of the data to determine what filters were needed to filter the power system related and other undesirable sinusoidal spectral content, and low-frequency trends from the data; (3) the needed filters were designed; (4) the data was filtered to remove the undesirable sinusoidal spectral content; (5) the data was then DC normalized; (6) the resulting filtered and DC normalized data was spectroscopically assessed to confirm filtering results and the time series data was plotted versus voltage; (7) the high-pass filter was applied to the data to remove all low-frequency trends leaving only the impulses in the data, and this filtered time series data was plotted as a function of voltage; and (8) the data was then passed to a thresholding process where the signal voltage level was compared to a threshold voltage level (positive and negative thresholds). Every time the signal voltage passed a threshold value a counter incremented a threshold value bin. This process generated a list of counts versus threshold that was used to determine the power trend through nonlinear regression and then the result was plotted. This process was applied to both drainage and imbibition data.

[13] Video recordings of displacements show that individual pore dewatering takes place in Haines jumps [*Lu et al.*, 1994]. Figure 2 shows for example Haines jumps during the drainage process for the sand used in the following experimental investigations. These pictures show that there are places where there are sudden jumps in the displacement of the meniscus during drainage while there are other areas were the position of the meniscus is stable over the same period of time.

3. Results and Discussion

[14] Drainage was begun by opening the control valve and terminated by closing the control valve (Figure 1). The phase preceding the drainage is labeled phase I below while phase II corresponds to the drainage experiment itself, and phase III corresponds to the postdrainage relaxation. Each phase has different electrical signatures (Figure 3). The channel by channel DC properties of the records were normalized in phase I, making most channel responses near zero in this region. This region is electrically characterized by relatively stable trends with a low RMS noise.

[15] The drainage region shows the expected self-potential trend as a positive voltage response during water table lowering (drainage). This low-frequency dynamic behavior was modeled recently by *Revil et al.* [2008]. However, bursts in the electrical potential were also observed on top of these expected low-frequency behaviors. The signals of most interest are the transient signals that are observed in this region. It should be noted that the drainage was started from a completely saturated sand volume (saturated to the surface), and the electrical characteristics at the beginning of the drainage are different from the electrical characteristics displayed later in the drainage process. The drainage region times of 10 to 25 s are electrically and acoustically quieter than later time sections. Since the water was drained through one port, it is expected that the water table will achieve a nonflat surface that is higher at the end farthest from the drain, and lowest directly above the drain. Enough water drains away from the surface by 30 s for the onset of the electrical and acoustic noise behavior of interest. This noisy behavior continues until drainage was terminated.

[16] The relaxation region (phase III) shows a significant DC offset with a negative trend on most channels, indicating that the water table surface is relaxing to a constant hydraulic potential surface. It can be seen in Figure 3 that data acquisition was terminated before relaxation was completed. It should be noted that the AC electrical and acoustic properties of this region are quiet except for a few straggling transient events (Figure 4). These straggling events suggest that the sand volume may be undergoing a localized process of consolidation during the relaxation of the water table.

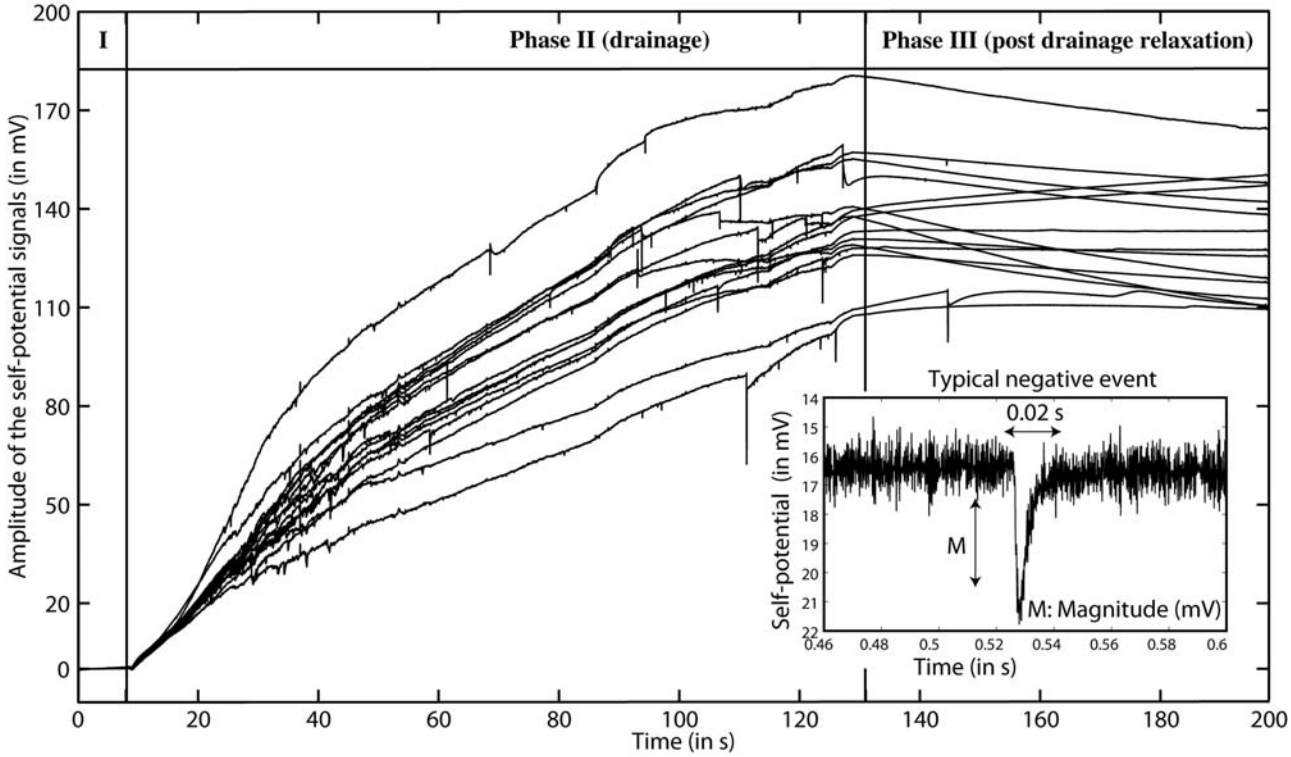

Figure 3. Electrograms for a selected set of channels. Phase I corresponds to the data recorded before starting the drainage. Phase II corresponds to the drainage experiment. Phase III corresponds to the postdrainage data and the relaxation of the water table. A typical negative event is shown in the inset (voltages are in mV). These anomalies are characterized by a drop in the electrical potential (characterizing the magnitude of the event) and a relaxation tail.

[17] Figure 3 shows how the signal characteristics change as drainage proceeds from being dominated by purely fluid flow to the invasion of air as it begins to enter pores initially containing water. In phase II, the noise clearly begins at a much lower level and increases dramatically with mostly negative excursions, which dominate as time increases (Figure 4). Phase II is dominated by a series of different types of electrical events, but most prominent are the negative voltage leading edge with a long (up to 1 s) tail. Most of the negative voltage spikes do not have a coincident signal offset; however, some of them show various types of offsets (Figure 3). The cause of the variety of these offsets has not been determined but could be suggestive of a localized process of consolidation of the sand near the lesser compacted surface or within the volume. Video recording show movement of sand grains near the surface during drainage lending support to the consolidation suggestion as an explanation of the observed signal offsets.

[18] Similar data have been obtained for an imbibition experiment (not shown here). However, the amplitude and the number of electrical bursts are observed to be both much smaller than for drainage. The most important events are

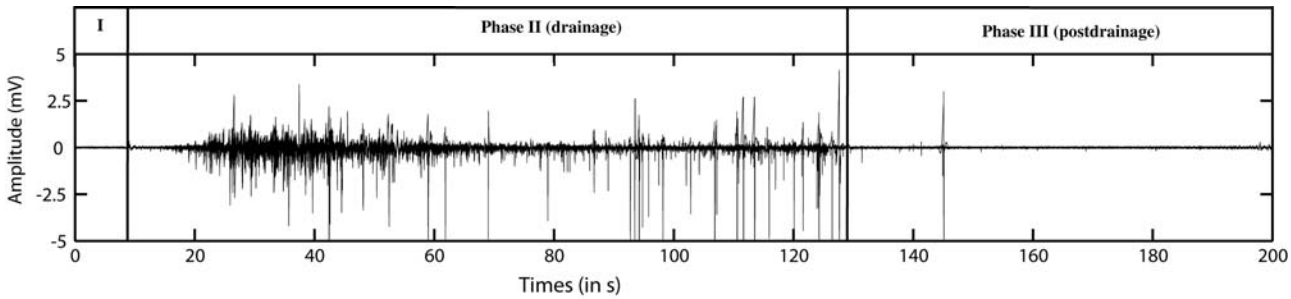

Figure 4. High-pass-filtered self-potential data showing the level of electrical noise produced during drainage. The full 195 s electrogram is shown. In phase II, the electrogram exhibits large negative voltage spikes with decaying tails. The negative voltage spikes typically involve only a few channels, implying that they are located not too far from these electrodes.

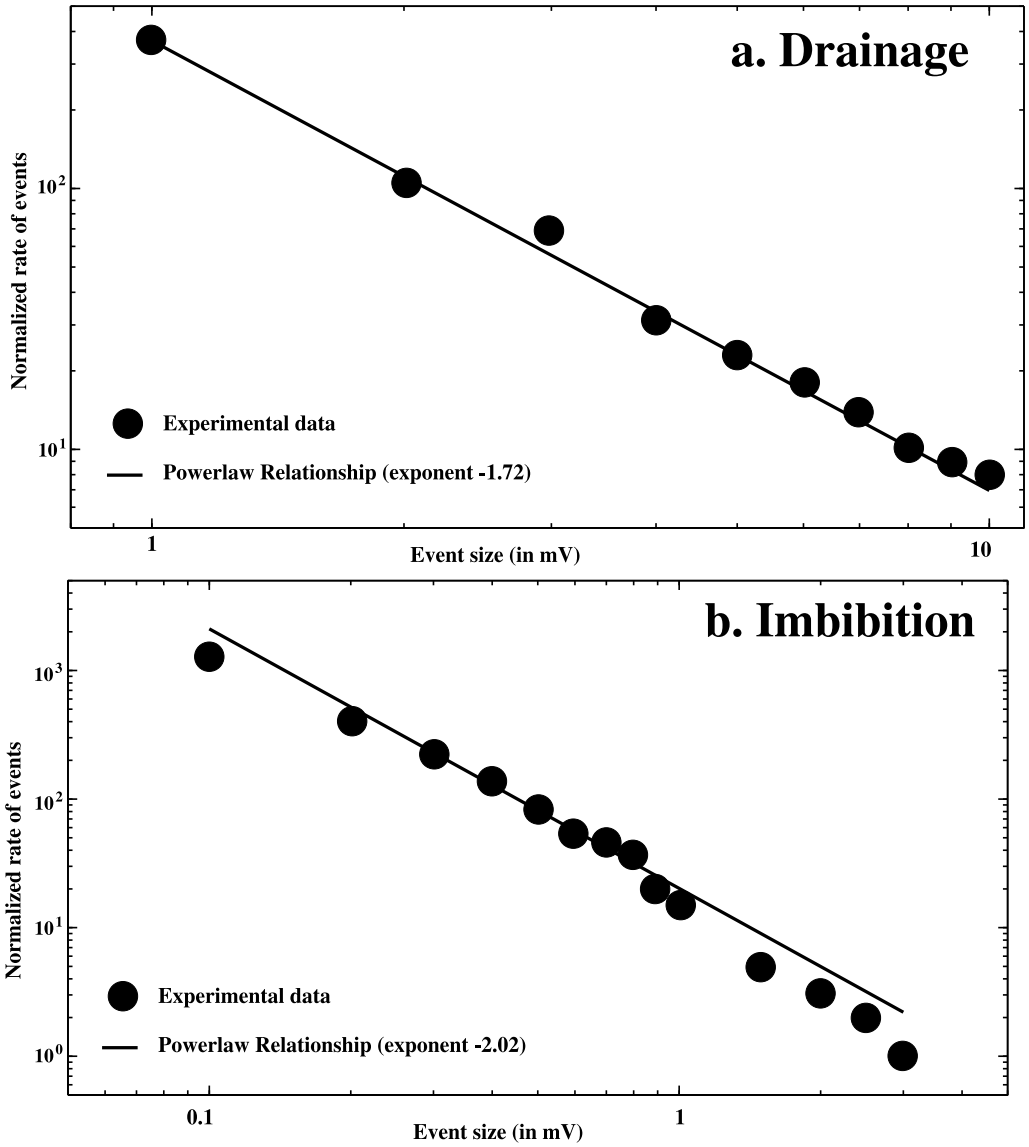

Figure 5. Frequency of electrical burst for both drainage and imbibition versus the magnitude of the events. (a) In the case of drainage, the data follow a power law distribution with a fitting exponent of -1.72. (b) The imbibition data show a drop off that is much faster with increasing event magnitude because fewer numbers of pores are involved in the formation of Haines jumps.

positive excursions in the self-potential signals. These observations are consistent with Haines jumps during imbibition described in section 2.

[19] As explained above, the sudden movement of the meniscus during drainage experiments has been documented in a number of studies [*Aker et al.*, 2000]. The invading fluid (air in the present case) is found to suddenly invade a larger region of the pore space. These bursts of flow (Haines jumps) are characterized by large fluctuations in the pore water pressure and acoustic emissions [*Sethna et al.*, 2001; *DiCarlo et al.*, 2003]. In our drainage experiment, crackling acoustic emissions were easily discerned by human ears and were heard at the same time that the electrical noise occurred. However, the acoustic and electrical noises phenomena have not been correlated yet. Haines jumps seem to be the source of the signals we observed.

[20] The difference in magnitude distributions for drainage and imbibition is a result of the difference in the types of pore-filling processes as explained in section 2. Figure 5 shows the number of events counted versus event magnitude for both drainage and imbibition. Note that the magnitude of the self-potential events is much larger on drainage than on imbibition. On drainage, the magnitude of the electric events shows a power law distribution with an exponent of -1.7 ± 0.1 fitting the data well over the complete range of event magnitudes. These results are in agreement with the seismic data analysis of *DiCarlo et al.* [2003] who also found a power law exponent of -1.7 ± 0.2.

[21] For imbibition, basically no large events are seen and the spectrum of event sizes drops off much steeper with a fit exponent of -2.0 ± 0.4 (the seismic data of *DiCarlo et al.* [2003] show an exponent of -2.6 ± 0.4). Additionally, our results are comparable with the pressure fluctuations modeled by *Aker et al.* [2000]. In their case, the pressure fluctuations have a power law distribution during slow drainage with a power law exponent of -1.9. It is interest-

ing to note that the Haines jump phenomenon works down to liquid helium temperatures. *Lilly et al.* [1996] observed avalanches in He4 at temperatures of about 1.5 K.

[22] Another possibility to explain the electrical fluctuations we observed would be that the observed electrical disturbances may result from the seismoelectric conversion of the seismic waves. This possibility can be dismissed because acoustic signals are typically on the order of 0.1 Pa [*DiCarlo et al.*, 2003]. With a typical streaming coupling coefficient of -10^6 V/Pa for tap water, the order of magnitude of the coseismic electrical signals would 10^{-4} mV, much below the amplitude of the signals we detected (above 0.1 mV).

4. Concluding Statements

[23] High-frequency monitoring of a drainage experiment reveals a complex dynamic behavior of the streaming potential response. In addition to the low-frequency dynamic behavior analyzed recently by *Revil et al.* [2008], a higher-frequency response was also observed. During imbibition experiments, the acoustic noise and electrical noise were reduced, although still present to a somewhat smaller degree. These electrical disturbances are consistent with Haines jumps. Self-organized critical systems that evolve in bursts (from landslides to earthquakes) predict that these types of systems should exhibit discrete impulsive events spanning a broad range of sizes with a power law behavior [*Sethna et al.*, 2001]; the analysis of our data shows that the electrical signals caused by the drainage of porous media is agreement with this. The use of self-potential localization methods [see *Crespy et al.*, 2008] could be used to locate these events inside the sandbox, and their use will be investigated in a future work. Electromagnetic emissions like the one described in the present study could be used to characterize percolation invasion processes in these systems when the discrete impulsive events result in pulse current events.

[24] **Acknowledgments.** We thank Dani Or for pointing us to this very interesting topic.

References

Aker, E., K. J. Maløy, A. Hansen, and S. Basak (2000), Burst dynamics during drainage displacements in porous media: Simulations and experiments, *Europhys. Lett.*, *51*, 55–61, doi:10.1209/epl/i2000-00331-2.

Crandall, D., G. Ahmadi, M. Ferer, and D. H. Smith (2009), Distribution and occurrence of localized-bursts in two-phase flow through porous media, *Physica A*, *388*, 574–584, doi:10.1016/j.physa.2008.11.010.

Crespy, A., A. Revil, N. Linde, S. Byrdina, A. Jardani, A. Bolève, and P. Henry (2008), Detection and localization of hydromechanical disturbances in a sandbox using the self-potential method, *J. Geophys. Res.*, *113*, B01205, doi:10.1029/2007JB005042.

DiCarlo, D. A., J. I. G. Cidoncha, and C. Hickey (2003), Acoustic measurements of pore-scale displacements, *Geophys. Res. Lett.*, *30*(17), 1901, doi:10.1029/2003GL017811.

Haines, W. B. (1930), Studies in the physical properties of soils. The hysteresis effect in capillary properties, and modes of moisture distribution associated therewith, *J. Agric. Sci.*, *20*, 97–116, doi:10.1017/S002185960008864X.

Jardani, A., A. Revil, A. Bolève, and J. P. Dupont (2008), Three-dimensional inversion of self-potential data used to constrain the pattern of ground water flow in geothermal fields, *J. Geophys. Res.*, *113*, B09204, doi:10.1029/2007JB005302.

Jardani, A., A. Revil, W. Barrash, A. Crespy, E. Rizzo, S. Straface, M. Cardiff, B. Malama, C. Miller, and T. Johnson (2009), Reconstruction of the water table from self potential data: A Bayesian approach, *Ground Water*, *47*(2), 213–227, doi:10.1111/j.1745-6584.2008.00513.x.

Leroy, P., A. Revil, S. Altmann, and C. Tournassat (2007), Modeling the composition of the pore water in a clay-rock geological formation (Callovo-Oxfordian, France), *Geochim. Cosmochim. Acta*, *71*(5), 1087–1097, doi:10.1016/j.gca.2006.11.009.

Lilly, M. P., A. H. Wootters, and R. B. Hallock (1996), Spatially extended avalanches in a hysteretic capillary condensation system: Superfluid 4He in nuclepore, *Phys. Rev. Lett.*, *77*(20), 4222–4225, doi:10.1103/PhysRevLett.77.4222.

Lu, T. X., J. W. Biggar, and D. R. Nielsen (1994), Water movement of glass bead porous media: 1. Experiments of capillary rise and hysteresis, *Water Resour. Res.*, *30*, 3275–3281, doi:10.1029/94WR00997.

Revil, A., C. Gevaudan, N. Lu, and A. Maineult (2008), Hysteresis of the self-potential response associated with harmonic pumping tests, *Geophys. Res. Lett.*, *35*, L16402, doi:10.1029/2008GL035025.

Sethna, J. P., K. A. Dahmen, and C. R. Myers (2001), Crackling noise, *Nature*, *410*, 242–250, doi:10.1038/35065675.

Tuller, M., and D. Or (2001), Hydraulic conductivity of variably saturated porous media: Film and corner flow in angular pore space, *Water Resour. Res.*, *37*(5), 1257–1276, doi:10.1029/2000WR900328.

A. Haas and A. Revil, Department of Geophysics, Colorado School of Mines, 1500 Illinois Street, Golden, CO 80401, USA. (arevil@mines.edu)